ISSN: 2319-8753

International Journal of Innovative Research in Science, Engineering and Technology

(An ISO 3297: 2007 Certified Organization)

Vol. 3, Issue 4, April 2014

Localizing 2-D Digital Skin Images Using SAVC Algorithm

J. Kavitha [1], Dr. D. Saravanan [2]

P.G. Student, Department of Computer Applications, Sathyabama University, Chennai-600119, Tamil Nadu, India[1]

Assistant Professor, Department of Computer Applications, Sathyabama University, Chennai-600119, Tamil Nadu, India[2]

Abstract: The skin disease namely psoriasis affects a large number of people in the country, there is a need for improvement in the field of therapeutics which would actually be able to cure the disease. Hence my work has been designed in order to use the segmented scaling images for enhancing the treatment for psoriasis. The approach is to reduce the problem of segmenting scaling to a binary classification problem by removing erythema from consideration and then classifying the remaining pixels as either skin pixels or scaling pixels. Thus there are two stages as said which are namely feature extraction stage and scaling segmentation stage. Feature extraction is done using gabor filter. Segmentation of scaling is done using training set from the filtered images. A Markov random field (MRF) is used to smooth a pixel-wise classification from a support vector machine (SVM) that utilizes a feature space derived from image colour and scaling texture.

Keywords: Feature extraction, image segmentation, Markov Random Field (MRF), psoriasis, Support Vector Machine (SVM).

I. INTRODUCTION

Psoriasis is a chronic skin disease that affects an estimated 125 million people worldwide. In this project, I have proposed a method of segmentation of scaling in 2-D psoriasis skin images. Here Markov Random field (MRF) is used to smooth a pixel-wise classification from a support vector machine (SVM) that utilizes a feature space derived from image colour and scaling texture. This method is expected to give reliable segmentation results when evaluated with images in different lighting conditions, skin types, psoriasis types. This system is believed to be the first to localize scaling directly in 2-D digital images.

The paper presents what we believe to be the first algorithm to automatically segment scaling directly from skin and erythema in 2-D digital images. The approach is to reduce the problem of segmenting scaling to a binary classification problem by removing erythema from consideration and then classifying the remaining pixels as either skin pixels or scaling pixels. The feature space used in the classification is derived from the colour contrast between scaling and erythema, and the image texture describing the roughness of scaling which is determined by the aggregated result from a bank of Gabor filters. Our evaluation indicates that our combination of Markov random fields (MRFs) with support vector machines using an appropriate feature space can solve a wide range of scaling segmentation problems that include variations in lighting conditions, variations in skin type and variations in the types of psoriatic lesions.

Scaling typically appears as white or creamy coloured scales on regions of red and inflamed skin (erythema) but can also appear in isolation without the accompanying erythema. When psoriasis appears without discernibly white or creamy flakes on normal skin. Scaling can present as small spots or as patches scattered within erythema. Fig. 1 shows some examples of the variation in the appearance of scaling. The variation makes it difficult to identify scaling boundaries through more conventional boundary detection algorithms and as a consequence we use a pixel based classification and labelling approach.

Moreover, the colour of scaling may be very similar to that of normal skin, especially if the skin is fair, making it difficult to differentiate between scaling and normal skin using on colour alone. However, the rough textured surface of scaling is markedly different from normal skin. The algorithm uses a feature space derived from both colour and texture to classify pixels. The result is a pipeline that is essentially a pixel labelling algorithm that identifies scaling in 2-D digital skin images without the need for locating psoriasis first. It is composed of two main stages: 1) a feature

ISSN: 2319-8753

International Journal of Innovative Research in Science, Engineering and Technology

(An ISO 3297: 2007 Certified Organization)

Vol. 3, Issue 4, April 2014

extraction stage and 2) a scaling segmentation stage. The two stages are the accompanying erythema it appears as described as follows (see Fig. 2).

Step 1) The algorithm first analyzes skin colour and skin texture using an appropriately chosen color space and bank of Gabor filters to create a feature space for the image.

Step 2) The algorithm next removes erythema pixels from consideration and resamples the image to collect training samples for the classification process. The segmentation is achieved by using a MRF and the hyperplane derived from a support vector machine (SVM).

II.RELATED WORK

TITLE: AUTOMATED FEATURE EXTRACTION FOR EARLY DETECTION OF DIABETIC RETINOPATHY IN FUNDUS IMAGES, X.ZHANG AND O. CHUTATAPE, SEPT. 1996.

Automated detection of lesions in retinal images can assist in early diagnosis and screening of a common disease: Diabetic Retinopathy. A robust and computationally efficient approach for the localization of the different features and lesions in a fundus retinal image is presented in this project. Since many features have common intensity properties, geometric features and correlations are used to distinguish between them. We propose a new constraint for optic disk detection where we first detect the major blood vessels first and use the intersection of these to find the approximate location of the optic disk. This is further localized using color properties. We also show that many of the features such as the blood vessels, exudates and microaneurysms and hemorrhages can be detected quite accurately using different morphological operations applied appropriately. These compare very favorably with existing systems and promise real deployment of these systems.

TITLE: THE DIARETDB1 DIABETIC RETINOPATHY DATABASE AND EVALUATION PROTOCOL, HEIKKI KALVIAINEN AND JUHANI PIETILA, 2002.

Automatic diagnosis of diabetic retinopathy from digital fundus images has been an active research topic in the medical image processing community. The research interest is justified by the excellent potential for new products in the medical industry and significant reductions in health care costs. However, the maturity of proposed algorithms cannot be judged due to the lack of commonly accepted and representative image database with a verified ground truth and strict evaluation protocol. In this study, an evaluation methodology is proposed and an image database with ground truth is described. The database is publicly available for benchmarking diagnosis algorithms. With the proposed database and protocol, it is possible to compare different algorithms, and correspondingly, analyze their maturity for technology transfer from the research laboratories to the medical practice.

TITLE: IMPROVING MICROANEURYSM DETECTION USING AN OPTIMALLY SELECTED SUBSET OF CANDIDATE EXTRACTORS AND PREPROCESSING METHODS,BALINT ANTAL, ANDRAS HAJDU, JANUARY 2012

In this project, I present an approach to improve microaneurysm detection in digital color fundus images. Instead of following the standard process which considers preprocessing, candidate extraction and classification, we propose a novel approach that combines several preprocessing methods and candidate extractors before the classification step. We ensure high flexibility by using a modular model and a simulated annealing-based search algorithm to find the optimal combination. Our experimental results show that the proposed method outperforms the current state-of-the-art individual microaneurysm candidate extractors.

III.MATERIALS AND METHODS

The work presented here consists of five modules: 1) Preprocessing 2) Feature Extraction 3) Removing erythema 4) Training sets collection and localization 5) Segmentation

ISSN: 2319-8753

International Journal of Innovative Research in Science, Engineering and Technology

(An ISO 3297: 2007 Certified Organization)

Vol. 3, Issue 4, April 2014

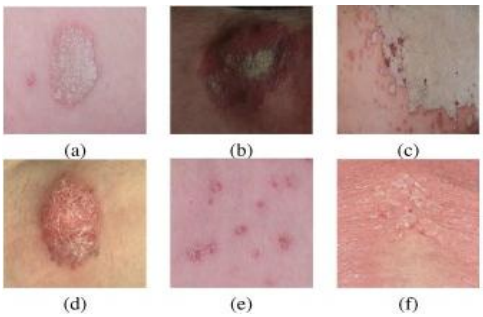

Fig.1 Examples of scaling in psoriasis lesions. (a) Scattered scaling in plaque psoriasis. (b) Patched scaling in plaque psoriasis. (c) Extensively covered scaling in plaque psoriasis. (d) Scaling in guttate psoriasis. (e) Scaling in pustular psoriasis. (f) Scaling in erythrodermic psoriasis.

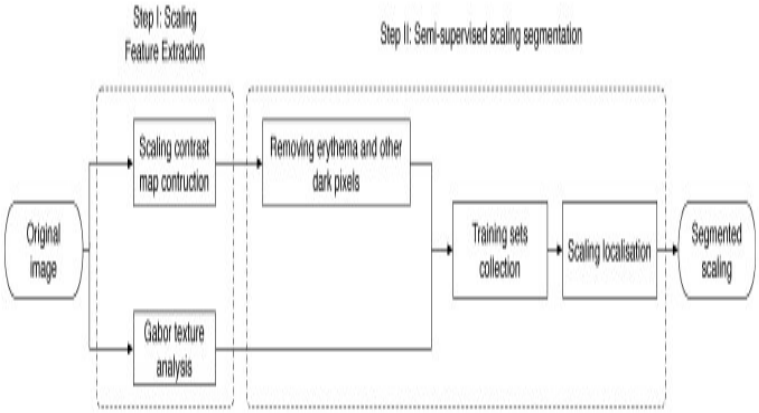

Fig. 2 Flowchart of the algorithm for automatic segmentation of scaling in 2-D psoriasis skin images.

1. Preprocessing:

Preprocessing is removal of noise contents present in the image. It is done using the preprocessing algorithm 'Scaling Contrast Map'. A scaling contrast map is developed to enhance the contrast of scaling from erythema. The map aims to enhance the contrast of scaling especially in situations where scaling is scattered in erythema.

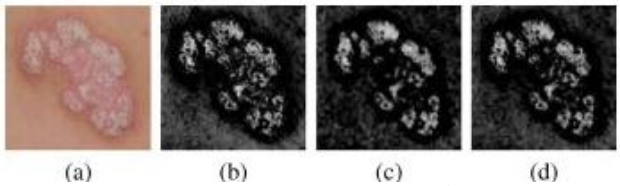

Fig. 3 Scaling contrast map construction. (a) Original image. (b) Contrast map derived from **L***. (c) Contrast map derived from **a***. (d) Scaling contrast map.

$\mathbf{L^*a^*b^*}$ color space is used to develop a pair of multi-scale center-surround filters that increase the contrast between scaling and erythema. The $\mathbf{L^*}$ dimension specifies lightness where an $\mathbf{L^*}$ value of 0 is black and an $\mathbf{L^*}$ value of 100 is a diffuse white. The $\mathbf{a^*}$ dimension is the red–green dimension, where a positive value of $\mathbf{a^*}$ is red and a negative value of $\mathbf{a^*}$ green, and the $\mathbf{b^*}$ dimension is the blue–yellow dimension, where a positive value of $\mathbf{b^*}$ is blue and a negative value of $\mathbf{b^*}$ is yellow.

The color of scaling correlates well with higher values of $\mathbf{L^*}$ and erythema with positive values of $\mathbf{a^*}$. Shadows result in smaller values but do not necessarily affect the other dimensions. Furthermore, by inverting the dimension the color difference between scaling and the surrounding erythema or skin can be increased. With this in mind a scaling contrast map can be defined as follows: $\mathbf{S_{x,y} = J(L^*_{x,y}) + J(inv(a^*_{x,y}))}$ where $\mathbf{S_{x,y}}$ is the value of scaling contrast filter **S** at the image coordinate **(x,y)**, **J(.)** is a multi-scale center-surround filter that detects contrast, and **inv($\mathbf{a^*}$)** inverts the image

ISSN: 2319-8753

International Journal of Innovative Research in Science, Engineering and Technology

(An ISO 3297: 2007 Certified Organization)

Vol. 3, Issue 4, April 2014

in the $\mathbf{a}^*$ dimension and is defined by $\mathbf{inv}(a^*_{x,y})=\mathbf{max}_{i,j}(a^*_{i,j}) - a^*_{x,y}$, where **(i,j)** runs through all the coordinates in the image.

2. Feature Extraction:

Feature extraction is extracting the number of important objects present in the image. Algorithm of extraction is Gabor Texture analysis. The algorithm uses a bank of 24 Gabor filters designed to respond well in a variety of skin and scaling texture conditions. Finally, the Gabor texture image is obtained by summing the smoothed output.

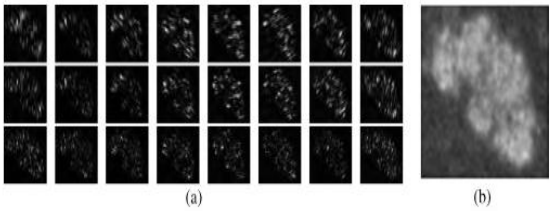

Fig. 4 Texture examination corresponding to the original image in Fig. 3. (a) Gabor filtering responses from a bank of Gabor filters (the spatial frequency changes along the row and the rotation angle changes along the column). (b) The final Gabor feature image.

TABLE 1
Parameters defining the bank of gabor filters used for scaling texture analysis

Spatial frequencies	$1/\lambda$	23, 31, 47 cycles per image
Rotation angles	θ	$0, \frac{\pi}{8}, \frac{\pi}{4}, \frac{3\pi}{8}, \frac{\pi}{2}, \frac{5\pi}{8}, \frac{3\pi}{4}, \frac{7\pi}{8}, \pi$
Phase shift	ψ	0
Spatial aspect ratio	γ	0.5

3. Removing erythema:

Take out the dark pixels representing erythema, hair, moles and other blemishes are removed using the scaling contrast map. The first step is to threshold out the dark pixels representing erythema, hair, moles and other blemishes using the scaling contrast map **S**. Scaling and normal skin pixels remain in consideration after the application of the contrast map because they result in a significantly high value of **S**. We define a binary image **M** by

$$M_{x,y} = \begin{cases} 1, & \text{if } S_{x,y} \geq t_x \\ 0, & \text{otherwise} \end{cases}$$

where $\mathbf{t_x}$ is the threshold for dark pixels. Pixels labelled with 1 are retained for further analysis while pixels labelled with 0 denote darker pigments and are removed from further consideration.

The scaling contrast map is applied to the image and the resulting image is processed to thresh-hold out all dark pixels representing darker pigments in the skin and including erythema, hair, moles, and other blemishes.

4. Training sets collection and localization:

The training set data is collected by following steps

a) Approximate Localization of Erythema

The location of erythema is identified by gray-scale intensity using the scaling contrast map where low values are indicating red pixels; normal skin would show negative values in the scaling contrast map.

The location of erythema is identified by gray-scale intensity using the scaling contrast map **S**

where low values **S** of indicate red pixels. A rough segmentation of erythema, but one that serves our purposes, can be obtained by empirically labelling a pixel to be erythema if $S_{x,y} \leq 0.2 \min_{i,j} S_{i,j}$. This is because darkened normal skin would show negative values in the scaling contrast map, but would still be greater than the values of erythema. For the purpose of determining the severity of psoriasis lesions we require a much more accurate segmentation of erythema than given here.

b) Obtaining a Sample of Scaling and Skin Pixels

Localization of erythema is to collect a sample of skin pixels and scaling pixels. Using the fact that scaling is often

ISSN: 2319-8753

International Journal of Innovative Research in Science, Engineering and Technology

(An ISO 3297: 2007 Certified Organization)

Vol. 3, Issue 4, April 2014

surrounded, or partially surrounded, by erythema, we use dilation and erosion operations to create regions of scaling enclosed by boundaries of erythema. Dilating by a disk **U** of radius ***p*** pixels widens each of the erythema regions. The **(θ)** algorithm erodes the erythema regions back to their original width while keeping the closed "doughnut" shape. The variable η is used for counting how many dilation phases have taken place so that we know how many erosion phases need to take place to regain the original erythema width (line 9, where η**U** is a disk-shaped structure with radius ηp).

c) Soft-Constrained K -Means Clustering

The algorithm uses a soft-constrained K-means clustering to select training data from the candidate sets. The constraints are defined as the probability of data being in each cluster in the initial stage. A cluster of scaling pixels C_1 and a cluster of skin pixels C_2 are formed from $\mathbf{L}_{scaling} \cup \mathbf{L}_{skin}$, and then within each of these clusters the pixels with the great likelihood of being scaling and normal skin respectively are chosen. The clustering algorithm partitions the feature set into the set of features into those that are closer to ∂_1 and those that are closer to ∂_2 with respect to the Euclidean norm $\|\cdot\|$.

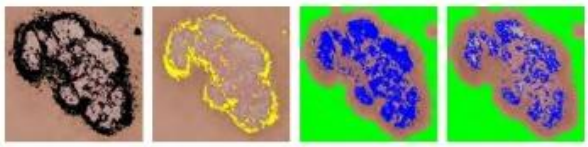

(a) (b) (c) (d)

Fig. 5 Stages in the collection of the training sets from the image shown in where dark colFig. 3. (a) Preprocessing using the scaling contrast filter ored pixels are in the matrix . (b) The approximate localization of erythema marked in yellow. (c) The candidate regions of scaling (marked in blue) and normal skin marked in green. (d) The representative training sets for scaling marked in blue and normal skin marked in green.

The training set $\mathbf{T}_i$ for the class $\mathbf{C}_i$ is taken to be those samples $\mathbf{L}_{x,y}$ in the image such that

$$\frac{W(L_{x,y}, C_i)\,\|F_{x,y} - O_i\|^2}{W(L_{x,y}, C_j)\,\|F_{x,y} - O_j\|^2} \leq t_h$$

where **j=2** if **i=1**and **j=1** if **i=2**. The threshold is chosen to be 0.1 in order to ensure that training samples have a high likelihood of being within their respective pixel classes.

The minimum of **h(C, ∂)** depends on the initial choice of centroids where a good choice is more likely to lead to a global minimum but poorer choices lead to local minimum. The initial centroids for the two classes are chosen to be the average of the following feature vectors.

- ∂_1(scaling) is the average of the feature vectors with high responses of the Gabor filter for the region $\mathbf{L}_{scaling}$.
- ∂_2(normal skin) is the average of the feature vectors with low responses of Gabor filter in the region $\mathbf{L}_{skin}$.

The threshold between high and low responses of the Gabor filter is determined by using Otsu thresholding. Fig. 5 visually illustrates the process of collecting training sets of scaling and normal skin from the skin image.

5. Segmentation:

Segmentation of scaling from normal skin using SVM (Support Vector Machine) and MRF (Markov Random Field) algorithms. SVM is to provide an initial classifier that the MRF then uses to smooth the region located by the SVM.

a) The Support Vector Machine

Let **F** be the feature set and $a_{x,y} \in \{1, -1\}$ be a set of class labels such that $a_{x,y} = -1$ means that the pixel at (x, y) belongs to the class of skin pixels while $a_{x,y} = 1$ means that the pixel at (x, y) belongs to the class of scaling pixels. SVMs are common technique for solving classification problems. The aim for the basic SVM is to find a hyperplane that separates a data set into one of two predefined classes. The hyperplane is defined using training data to estimate the hyperplane parameters so that the distance to any training sample is maximized.

b) The Markov Random Field to Classify Pixels

SVMs can be used to solve a wide class of scaling from skin segmentation problems. However, when scaling and normal skin occur at psoriasis lesion boundaries, the classification more often depends on the image structure and the neighbourhood of the pixel being classified than on clear distinctions in feature space. An MRF is formulated precisely with this type of problem in mind. The proposed algorithm generates an SVM to provide an initial classifier that the

ISSN: 2319-8753

International Journal of Innovative Research in Science, Engineering and Technology

(An ISO 3297: 2007 Certified Organization)

Vol. 3, Issue 4, April 2014

MRF then uses to smooth the region located by the SVM.

Let $A = \{(S_{x,y}, T_{x,y}) | M_{x,y} = 1\}$ be the set of features for all of the image pixels that are not erythema pixels. The image is viewed as a hidden labelling process that results in a segmentation ω of the scaling pixels from the skin pixels through an observable set of image features for the nonerythema pixels. We seek a segmentation ω that maximizes the probability of obtaining the image features in ***A***.

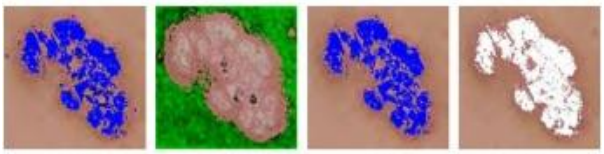

(a) (b) (c) (d)

Fig. 6 The segmentation of scaling for the lesion in Fig. 3. (a) The distance of a scaling pixel to the SVM hyperplane where darker pixels are closer to the SVM hyperplane. (b) The distance of normal skin pixels to the SVM hyperplane where darker green pixels are closer to the SVM hyperplane. (c) SVM-based MRF localization of scaling marked in blue. (d) Ground truth of scaling marked in white colour.

The objective function of the MRF is now defined as, $\omega = \arg\max P(A|\omega)P(\omega)$ where $P(A|\omega)$ is normally assumed to follow a Gaussian distribution but using the SVM in place of the Gaussian defines a distribution that already matches a good classification of skin and scaling pixels. The term $P(A|\omega)$ can be given as

$$P(A|\omega) = \prod_{x,y} P(A_{x,y}|\omega_{x,y})$$

where

$$P(A_{x,y}|\omega_{x,y}) = \begin{cases} \frac{1}{1+\exp(-d(A_{x,y}))}, & \text{if } a_{x,y} = \omega_{x,y} \\ \frac{\exp(-d(A_{x,y}))}{1+\exp(-d(A_{x,y}))}, & \text{otherwise} \end{cases}.$$

The probability $P(A_{x,y}|\omega_{x,y})$ is derived from the distance of $\boldsymbol{A}_{x,v}$ to the SVM hyperplane. The distance $\boldsymbol{d}(\boldsymbol{A}_{x,y})$ is given by

$$\begin{aligned} d(A_{x,y}) &= |\mathbf{w} \cdot \Phi(A_{x,y}) + b| \\ &= \left| \sum_{x',y'} a_{x',y'} \omega_{x',y'} \Phi(F_{x',y'}) \Phi(A_{x,y}) + b \right| \\ &= \left| \sum_{x',y'} a_{x',y'} \omega_{x',y'} K(F_{x',y'}, A_{x,y}) + b \right| \end{aligned}$$

where $a_{x,y}$ is a Lagrange multiplier. This distribution assigns a higher probability to $\mathbf{P}(\boldsymbol{A}_{x,y}| \omega_{x,y})$ if the class label for $\omega_{x,y}$ is the same as that given by the SVM.

Moreover, the probability for label $\omega_{x,y}$ is higher if it is further away from the hyperplane. Conversely, $\mathbf{P}(\boldsymbol{A}_{x,y}| \omega_{x,y})$ is assigned a lower probability if it is in a different class to that given by the SVM.

I. SIMULATION & RESULTS

The algorithm has been tested on a set of 103 images, which are collected from a dataset containing 722 psoriasis scaling images. The images were chosen so that there was a good distribution of images taken under different lighting conditions and at different angles, images with shadows, images with wrinkles, and images with hair. The images in each category were randomly

TABLE II
CLUSTERING METHOD COMPARISON

	MAD of skin	MAD of scaling	SS
K-means	0.0231	0.6045	0.0889
Fuzzy C-means	0.1873	0.8846	0.0220
Soft-constrained K-means	0.0110	0.6092	0.4598

ISSN: 2319-8753

International Journal of Innovative Research in Science, Engineering and Technology

(An ISO 3297: 2007 Certified Organization)

Vol. 3, Issue 4, April 2014

MAD values closer to 0 indicate a better training set, and SS values closer to 1 indicate a better training set. Table II hows the analysis results. For skin, the soft-constrained K-means has a better MAD value than the traditional K-means and the Fuzzy C-means. For scaling, the soft-constrained K-means shows an obvious advantage to the Fuzzy C-means in their MAD, but a slight inferiority to the K-means. Moreover, the soft constraints K-means has a much better SS over both the skin and scaling clusters.

TABLE III

COMPARISON OF SCALING SEGMENTATION RESULTS FOR IMAGES UNDER A VARIETY OF DIFFERENT CONDITIONS USING MANUALLY SELECTED TRAINING SETS

	Sensitivity	Specificity	Dice
Images with shadows			
SVM	0.8048	0.8734	0.4265
MRF	0.8334	0.8502	0.3995
Proposed method	0.8179	0.8707	0.4505
Images with wrinkles			
SVM	0.7303	0.8347	0.5180
MRF	0.7653	0.8019	0.5010
Proposed method	0.7278	0.8849	0.5503
Images with hair			
SVM	0.7334	0.9009	0.4427
MRF	0.7273	0.8426	0.3954
Proposed method	0.7591	0.8769	0.4737
Images about changes of imaging direction			
SVM	0.8264	0.8255	0.3747
MRF	0.7176	0.6444	0.2351
Proposed method	0.8035	0.8855	0.4398
Images about changes of illuminance			
SVM	0.7948	0.8225	0.3291
MRF	0.7370	0.8271	0.2739
Proposed method	0.7830	0.9112	0.4001

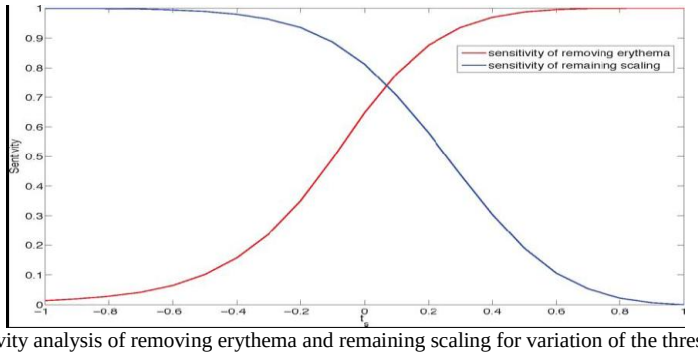

Fig. 7 Sensitivity analysis of removing erythema and remaining scaling for variation of the threshold value .

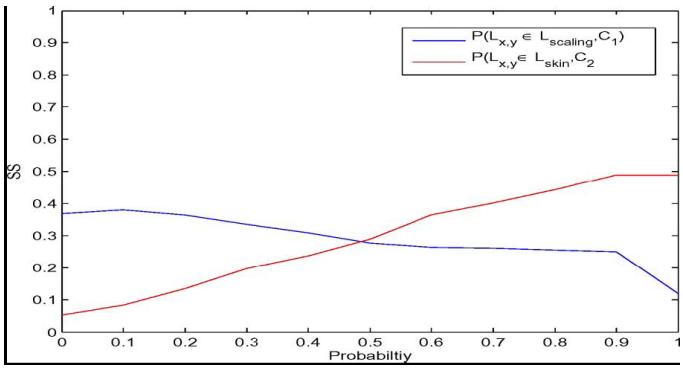

Fig. 8 SS analysis of variation of the probability in the soft-constrained K-means

II. CONCLUSION

In this paper, we present a general framework for automatic localizing scaling in psoriasis images. The result indicates that our algorithm makes progress towards the aim of automatic scaling segmentation. Scaling localization is

ISSN: 2319-8753

International Journal of Innovative Research in Science, Engineering and Technology

(An ISO 3297: 2007 Certified Organization)

Vol. 3, Issue 4, April 2014

implemented by a semi-supervised classification in this study. Two features are used: one is the scaling contrast map, which enhances the conspicuousness of scaling against erythema, and the other is a Gabor feature, which differentiates between scaling and normal skin based on image texture. Training sets for the classification are collected by a soft-constrained K-means to avoid the human interference. At the end, we combine the advantages of the SVM and the MRF to separate scaling from skin images. The SVM shows good performance in classification, but does not involve spatial information. Normal skin pixels around psoriatic lesion boundaries exhibit similar misclassified by the SVM. By integrating the SVM into our adaptation of the MRF, the internal structure of images are considered and that increases the classification accuracy. When we compare the algorithm to manually collected training sets, the proposed method presents a slightly weaker sensitivity to the SVM and the MRF. In the future, we will further investigate the algorithms for training set collection to improve the classification results. Moreover, scaling features need to be researched further, especially for the very vague scaling, which remains difficult to be detected using the algorithm in this paper.

REFERENCES

[1] Achanta R, Estrada F. J., Wils P., and Süsstrunk S., "Salient region detection and segmentation", in *Proc. Int. Conf. Comput. Vis. Syst.*, pp. 66–75, 2008.

[2] D.Saravanan, Dr.S.Srinivasan, "Data Mining Framework for Video Data", In the Proc.of International Conference on Recent Advances in Space Technology Services & Climate Change (RSTS&CC-2010), held at Sathyabama University, Chennai, Pages 196-198, November 13-15, 2010.

[3] D.Saravanan, Dr.S.Srinivasan, "Matrix Based Indexing Technique for Video Data ", International journal of Computer Science", 9 (5): 534-542, pp 534-542, 2013.

[4] Kato Z. and Chuen Pong T., "A Markov random field image segmentation model for color textured images," *Image Vis. Comput.*, vol. 24, pp. 1103–1114, 2006.

[5] Busse K. and John Koo M., "Residents' reports: Goeckerman combination therapy with low dose acitretin for HCV-associated psoriasis", Practical Dermatol., pp. 25–26, Apr. 2010.

[6] De Kerkhof P. V. and Kragballe K., "Psoriasis: Severity assessment in clinical practice. Conclusions from workshop discussions and a prospective multicentre survey of psoriasis severity," Eur. Dermatol J., vol. 16, no. 2, pp. 167–171, Mar. 2006.

[7] Delgado D., Ersboll B., and Carstensen J.M., "An image based system to automatically and objectively score the degree of redness and scaling in psoriasis lesions," in *Proc. 13th Danish Conf. Image Anal. Pattern Recognit.*, pp. 130–137, 2004.

[8] Grigorescu S. E., Petkov N., and Kruizinga P., "Comparison of texture features based on Gabor filters," *IEEE Trans. Image Process.*, vol. 11, no. 10, pp. 1160–1167, Oct. 2002.

[9] Jain A. K. and Farrokhnia F., "Unsupervised texture segmentationusing Gabor filters," *Pattern Recognit.*, vol. 24, pp. 1167–1186, 1991.

[10] Kato Z. and Chuen Pong T., "A Markov random field image segmentation model for color textured images," *Image Vis. Comput.*, vol. 24, pp. 1103–1114, 2006.

[11] Kruizinga P. and Petkov N., "Nonlinear operator for oriented texture," *IEEE Trans. Image Process.*, vol. 8, no. 10, pp. 1395–1407, Oct. 1999.

[12] Ma L. and Staunton R. C., "Optimum Gabor filter design and local binary patterns for texture segmentation," *Pattern Recognit. Lett.*, vol. 29, pp. 664–672, 2008.

[13] Meier M. and Sheth P.B., "Clinical spectrumand severity of psoriasis," Curr. Probl. Dermatol., vol. 38, pp. 1–20, 2009.

[14] Paul C., Gourraud P.A., Bronsard V., Prey S., Puzenat E., Aractingi S., Aubin,M. Bagot F., Cribier B., Joly P., Jullien D., Le Maitre M., Richard-Lallemand M.-A., and Ortonne J.-P., "Evidence-based recommendations to assess psoriasis severity: Systematic literature review and expert opinion of a panel of dermatologists," Eur J. Acad. Dermatol. Venereol., vol. 24, pp. 2–9, 2010.

[15] D.Saravanan, Dr.S.Srinivasan, "Video Image Retrieval Using Data Mining Techniques "Journal of Computer Applications, Volume V, Issue No.1, Pages39-42. ISSN: 0974-1925, Jan-Mar 2012.

[16] D.Saravanan, Dr.S.Srinivasan, " A proposed New Algorithm for Hierarchical Clustering suitable for Video Data mining.", International journal of Data Mining and Knowledge Engineering", Volume 3, Number 9, Pages 569, July 2011.